

# Influence of Conductive Heat-Losses on the Propagation of Premixed Flames in Channels

J. DAOU

*Department of Mathematics, UMIST, Manchester M60 1QD, UK*

and

M. MATALON\*

*Engineering Sciences and Applied Mathematics, McCormick School of Engineering and Applied Science, Northwestern University, Evanston, IL 60208-3125, USA*

We study the propagation of premixed flames in two-dimensional channels accounting for heat-losses by conduction to the channel's walls and a prescribed Poiseuille flow. A diffusive-thermal model is used and the calculations reported are based on Arrhenius-type chemistry. Attention is focused on the influence of the magnitude of heat losses, the channel width, and the mean flow velocity. Special attention is devoted to the determination of the global burning rate and to extinction conditions. Depending on the channel width we discuss two possible modes of extinction: total flame extinction brought about in narrow channels by excessive losses, and partial flame extinction near the walls of wider channels. Our predictions of the quenching distance, namely the smallest channel's width that permits flame propagation, and the dead space in the case of partial extinction are in agreement with experimentally reported values. The sensitivity of the flame to an imposed flow, being directed either towards the fresh mixture or towards the burned gas, is examined with some details.

© 2002 by The Combustion Institute

## INTRODUCTION

Flame propagation in channels is of great interest with applications in many practical combustion devices. The flame behavior near the walls of a channel, or a tube, plays an important role affecting the burning efficiency, quenching, or emission of chemical pollutants. For example, the gas flowing into crevice volumes of an internal combustion engine—small volumes with narrow entrances—cools by heat transfer to a temperature that may or may not allow the approaching flame to penetrate the crevice, with potential contribution to unburned hydrocarbon emissions [1]. As a result of heat loss the flame stands away from the wall with the quenching region about six times the laminar flame thickness; c.f. [2, 3]. Heat losses to the rim also play a crucial role in sustaining a stationary flame at the exit of a Bunsen burner, with the tendency for flashback diminished by increasing the heat losses. The orientation of a flame near a wall is, in general, determined by many factors that are not all well understood. Most studies, however, address the two particular cases where

the direction of flame propagation is either nearly parallel or normal to the wall. It is the first configuration which is relevant to the present study and several experiments have been carried out to simulate this condition [3–5]. An early theoretical investigation of this configuration, in absence of flow, was carried out by Von Karman and Milan [2], for cold wall conditions. Using a semi-analytical approach they computed flame shapes and predicted that the quenching distance is nearly 1.25 the planar adiabatic flame thickness. This is somewhat smaller than the values predicted experimentally which, as indicated earlier, is about six. In narrower tubes, total flame extinction is expected [6], but the boundary between the total extinction regime and partial extinction in the vicinity of the walls is not well determined in the literature.

In the present work we examine the problem of flame propagation in a (two-dimensional) channel of arbitrary width, accounting for heat losses by conduction to the walls. The ratio of the width of the channel to the laminar flame thickness is treated as a parameter and the magnitude of heat losses is varied from near adiabatic to cold-wall conditions, to cover the

\* Corresponding author. E-mail: matalon@nwu.edu

different situations that are typically encountered in applications. Propagation in a quiescent mixture as well as in the presence of an imposed flow, being directed from the unburned towards the burned gases or vice-versa, is considered, with the mean flow rate treated as a parameter. The solution of the Navier-Stokes equations coupled to the diffusion and energy equations with finite-rate chemistry, for the two-dimensional problem of flame propagation in a channel spanning the whole range of parameters that are being considered, is a formidable task. Instead, we use a diffusive-thermal model and, when an imposed flow is considered, assume a prescribed Poiseuille flow. Our objective is to determine the structure and characteristics of the two-dimensional flames that can propagate in a channel of specified width, when heat losses to the walls are accounted for. In a recent publication [7] we have addressed the same problem but only under adiabatic conditions. The only similar study reported in the literature [8], also based on a diffusive-thermal model, was able to produce results for few parameter values only, and without an imposed flow; the limited results are possibly because of the limited computing ability at the time.

The constant-density assumption adopted here is far from being trivial. Thermal-expansion induces a transverse flow that distorts the parabolic nature of the Poiseuille flow, with possible consequences on the propagation rate and other flame characteristics. Nevertheless, by discarding any coupling between the reactive and diffusive effects from the gas flow (c.f. [9]), sufficient qualitative insight into the effects of heat losses and of an imposed flow on flame propagation, can still be obtained. We identify two modes of extinction: total extinction in narrow channels and partial extinction in wider channels. We find that heat conduction to the walls plays a crucial role when the channel's width is not too large. In particular we identify the extent of the dead space, defined as the distance near the wall where the flame is quenched, and its dependence on the channel's width and the magnitude of heat losses. In narrow tubes total flame extinction is expected, conditions that are usually associated with flammability limits. In this case, we identify the quenching distance, corresponding to the small-

est channel's width that permits flame propagation.

The case of narrow channels is also treated asymptotically showing how the classical result of extinction by volumetric heat loss can be properly applied to a channel where the heat transfer occurs by conduction to the walls. In particular, the theory provides the proper scaling law for the channel's width—heat loss combinations and the shape of the two-dimensional flame front propagating with or against the flow. Finally, the numerical calculations which extend these results to wider channels, are seen to agree well with the asymptotic results which remain valid even for moderate channel's widths.

The channel's walls in this study are assumed non-catalytic and, in general, non-adiabatic. If the outer surface is maintained at the temperature of the fresh mixture  $T_u$  an appropriate boundary conditions for the temperature  $T$  is

$$\frac{\partial T}{\partial n} = K(T - T_u) \quad (1)$$

where  $K$  is a heat transfer parameter and  $n$  the distance measured in the direction normal to the wall. The limiting cases of adiabatic and cold isothermal walls are obtained when  $K = 0$  and  $K = \infty$ , respectively. Adiabatic walls are non-trivial to achieve in applications and cooling to the ambient temperature  $T_u$  must be provided to achieve the cold-wall boundary conditions. In practice, the heat flux to the walls of a combustion chamber varies substantially with location and may be better approximated by condition (1). It may be possible, for example, to estimate from the present results the wall temperature that permits flame propagation in a crevice of given diameter. We note that the alternative isothermal condition  $T = T_w$ , with  $T_w \neq T_u$ , used in [10] requires dealing with the cold-boundary difficulty by introducing, for example, an artificial cutoff temperature. The condition (1) does not necessitate such artificial resolution and permits retaining the Arrhenius-dependence of the reaction rate without modification.

After a brief description of the mathematical formulation (for more details see [12]), we present, an asymptotic analysis for the case of narrow channels followed with a numerical

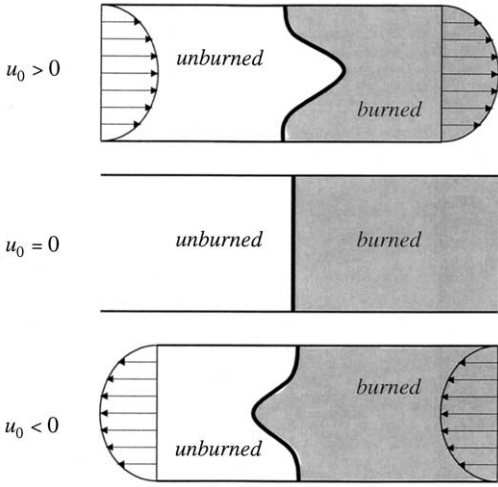


Fig. 1. Schematic of a premixed flame propagating in a channel under a prescribed Poiseuille flow, with the centerline velocity denoted by  $u_0$ .

study for moderate and wide channels. The case of no flow is considered first and used as reference for examining the influence of a flow on flame propagation. Finally, we treat the cold-walls boundary conditions separately; this case is the other extreme of adiabatic walls considered in our previous publication [7].

**FORMULATION**

A combustible gas is flowing in a two-dimensional infinitely long channel of width  $2a$ , as shown in Fig. 1. The flow in the channel is driven by a prescribed pressure gradient and is given by

$$v = \tilde{u}_0(1 - \tilde{y}^2/a^2)i, \quad -a < \tilde{y} < a$$

where  $\tilde{u}_0$  is the centerline velocity and  $i$  a unit vector along the  $\tilde{x}$ -axis. The flow may be either directed to the right with  $\tilde{u}_0 > 0$ , or to the left with  $\tilde{u}_0 < 0$ . Our objective is to describe the structure and speed of the two-dimensional deflagration wave that travels along the  $\tilde{x}$ -axis, separating the fresh cold mixture far to the left from the hot combustion products far to the right. As noted in the introduction, we neglect the effects due to thermal expansion and consider a diffusive-thermal or “constant-density” model.

The chemical activity is described by a one-

step overall reaction which consumes the fuel, assumed to be deficient, at a rate given by an Arrhenius law with  $B$  and  $E$ , the pre-exponential factor and activation energy, respectively. In such lean mixtures it is sufficient to follow the consumption of the fuel, since changes in the oxidizer’s concentration does not affect the reaction rate significantly. We select as a unit length the half-width of the channel  $a$  and as a unit speed the laminar flame speed

$$S_L = (2L_F B D_{th}/\beta^2)^{1/2} \exp(-E/2R^0 T_a).$$

Here  $T_a = T_u + QY_{F_u}/c_p$  is the adiabatic flame temperature with  $Q$  the total heat released by the chemical reaction, and  $T_u, Y_{F_u}$  the temperature and mass fraction of fuel in the fresh mixture. In addition,  $R^0$  is the universal gas constant,  $c_p$  is the specific heat (at constant pressure) of the mixture,  $L_F = D_{th}/D_F$  is the Lewis number with  $D_{th}$  and  $D_F$  representing, respectively, the thermal and mass diffusivities, and  $\beta \equiv E(T_a - T_u)/R^0 T_a^2$  is the Zeldovich number. The expression for  $S_L$  is based on the asymptotic approximation for  $\beta \gg 1$ . In terms of the normalized mass fraction  $y_F = Y_F/Y_{F_u}$  and temperature  $\theta = (T - T_u)/(T_a - T_u)$ , the non-dimensional governing equations, written in a frame of reference attached to the flame, are

$$[U + u_0(1 - y^2)] \frac{\partial y_F}{\partial x} = \epsilon L_F^{-1} \nabla^2 y_F - \epsilon^{-1} \omega \quad (2)$$

$$[U + u_0(1 - y^2)] \frac{\partial \theta}{\partial x} = \epsilon \nabla^2 \theta + \epsilon^{-1} \omega \quad (3)$$

where  $U$  is the propagation speed taken positive when the flame travels to the left, and  $\epsilon = \ell_F/a$  is the ratio of the laminar flame thickness  $\ell_F = D_{th}/S_L$  to half the channel-width  $a$ . (Note that when the same symbols are used, those with the  $\sim$  decoration denote dimensional quantities.) The reaction rate is given by

$$\omega = \frac{1}{2L_F} \beta^2 y_F \exp \left\{ \frac{\beta(\theta - 1)}{1 + \alpha(\theta - 1)} \right\}$$

with  $\alpha \equiv (T_a - T_u)/T_a$  being the heat-release parameter.

Far in the unburned gas, the chemistry is assumed frozen (because of a sufficiently large  $\beta$ ) so that the fuel mass fraction and the temperature take their prescribed values, namely

$$y_F = 1, \quad \theta = 0 \quad \text{as } x \rightarrow -\infty \quad (4)$$

Far in the burned gas all properties must become uniform, so that

$$\frac{\partial y_F}{\partial x} = \frac{\partial \theta}{\partial x} = 0 \quad \text{as } x \rightarrow +\infty. \quad (5)$$

Condition (1) and the no-flux condition for the mass fraction at the walls, together with the symmetry conditions along the channel-axis imply that

$$\frac{\partial \theta}{\partial y} = -\frac{k\theta}{\beta}, \quad \frac{\partial y_F}{\partial y} = 0 \quad \text{at } y = 1 \quad (6)$$

$$\frac{\partial \theta}{\partial y} = \frac{\partial y_F}{\partial y} = 0 \quad \text{at } y = 0 \quad (7)$$

where  $k/\beta = aK$ . The insertion of the dimensionless scaling factor  $\beta$  has been made solely for convenience. It enables comparison with the classical large activation energy result of a planar flame with volumetric heat losses which, as described below, is relevant to the case of narrow channels. Its introduction should not be interpreted as if the heat transfer coefficient in the boundary conditions depends on the chemistry of the mixture.

The total burning rate

$$\Omega \equiv \frac{1}{2\epsilon} \int_{-1}^1 \int_{-\infty}^{\infty} \omega dy dx,$$

representing the mass of fuel consumed per unit time relative to that consumed by a planar flame propagating in the same channel, may be obtained by integrating Eq. 2 across the channel and using the boundary conditions Eqs. 4 through 6. One finds

$$\Omega = \left( U + \frac{2}{3} u_0 \right) (1 - y_{F_\infty}) \quad (8)$$

where  $y_{F_\infty}$  is the residual mass fraction of fuel at  $x = \infty$ . Under adiabatic conditions all the available fuel is consumed at the flame and  $y_{F_\infty} = 0$ . In the presence of heat losses the temperature of the gas near the walls drops allowing for fuel to leak into the burned gas. The residual fuel typically burns behind the flame as it mixes with

the hot products and is totally depleted within a short distance. However, when there are excessively large heat losses that generate a rapidly decaying temperature behind the flame, the chemical reaction becomes extremely small (and practically negligible) behind the flame<sup>1</sup> which necessitates carrying the calculation to extremely large distances to achieve complete reactant depletion. At any reasonable distance behind the flame, there will be residual fuel with  $y_{F_\infty} \neq 0$ . The problem thus possesses two eigenvalues: the propagation speed  $U$  and the residual mass fraction of fuel  $y_{F_\infty}$ ; for prescribed conditions, a solution of Eqs. 2 through 6 exists only for particular values of  $U$  and  $y_{F_\infty}$ . The burning rate  $\Omega$  can then be deduced from Eq. 8.

## NARROW CHANNELS-ASYMPTOTIC RESULT

We consider first the limit  $\epsilon \gg 1$ , which corresponds to a channel much narrower than the thickness  $\ell_F$  of a planar adiabatic flame. This necessitates rescaling the axial coordinate by writing  $\xi = x/\epsilon$ , so that the unit length in this direction is now  $\ell_F$  instead of  $\alpha$ . The governing Eqs. 2 and 3 take the form

$$\begin{aligned} [U + u_0(1 - y^2)] \frac{\partial y_F}{\partial \xi} \\ - L_F^{-1} \left( \frac{\partial^2 y_F}{\partial \xi^2} + \epsilon^2 \frac{\partial^2 y_F}{\partial y^2} \right) = -\omega \end{aligned} \quad (9)$$

$$[U + u_0(1 - y^2)] \frac{\partial \theta}{\partial \xi} - \frac{\partial^2 \theta}{\partial \xi^2} - \epsilon^2 \frac{\partial^2 \theta}{\partial y^2} = \omega \quad (10)$$

with the same boundary conditions as before, except that  $x$  is now replaced by  $\xi$ .

We first note that by integrating the energy equation (10) across the channel one finds that

<sup>1</sup>For finite values of  $\beta$  the reaction rate does not vanish identically no matter how small  $\theta$  is, a reminiscent of the "cold boundary difficulty"; the chemical reaction therefore proceeds until *all* the fuel is consumed. For realistic values of the activation energy, however, the reaction rate is exponentially small, and hence negligible, when  $\theta$  becomes sufficiently small. For the values  $\beta = 8$  and  $\alpha = 0.85$  considered here the reaction rate is  $\approx 10^{-12}$  for  $\theta = 0.1$ , and  $\approx 10^{-24}$  when  $\theta = 0$ .

$$\Omega = \frac{\epsilon^2 \kappa}{\beta} \int_{-\infty}^{\infty} \theta(\xi, 1) d\xi \tag{11}$$

where used has been made of the fact that, for  $\kappa \neq 0$ , the temperature  $\theta$  vanishes as  $x \rightarrow \infty$ . This relation implies that, in the large  $\epsilon$  limit, the product  $k\epsilon^2 \equiv \kappa$  must be of order unity.

To leading order we find that

$$\frac{\partial^2 y_F}{\partial y^2} \sim 0, \quad \frac{\partial^2 \theta}{\partial y^2} \sim 0$$

which imply that the solution must be of the form

$$\theta = \bar{\theta}(\xi) + \epsilon^{-2} \theta'(\xi, y) + \dots$$

$$y_F = \bar{y}_F(\xi) + \epsilon^{-2} y'_F(\xi, y) + \dots$$

To the next order we have

$$L_F^{-1} \frac{\partial^2 y'_F}{\partial y^2} = \left\{ [U + u_0(1 - y^2)] \frac{d\bar{y}_F}{d\xi} - L_F^{-1} \frac{d^2 \bar{y}_F}{d\xi^2} + \bar{\omega} \right\}$$

$$\frac{\partial^2 \theta'}{\partial y^2} = \left\{ [U + u_0(1 - y^2)] \frac{d\bar{\theta}}{d\xi} - \frac{d^2 \bar{\theta}}{d\xi^2} - \bar{\omega} \right\},$$

where  $\bar{\omega}$  is the reaction rate based on  $\bar{y}_F$  and  $\bar{\theta}$ , together with the conditions

$$\frac{\partial \theta'}{\partial y} = \frac{\partial y'_F}{\partial y} = 0 \quad \text{at } y = 0$$

$$\frac{\partial y'_F}{\partial y} = 0, \quad \frac{\partial \theta'}{\partial y} = -\frac{\kappa \bar{\theta}}{\beta} \quad \text{at } y = 1.$$

Integrating once using the symmetry condition, yields

$$L_F^{-1} \frac{\partial y'_F}{\partial y} = \left[ (U + u_0) \frac{d\bar{y}_F}{d\xi} - L_F^{-1} \frac{d^2 \bar{y}_F}{d\xi^2} + \bar{\omega} \right] y - u_0 \left( \frac{d\bar{y}_F}{d\xi} \right) \frac{y^3}{3} \tag{12}$$

$$\frac{\partial \theta'}{\partial y} = \left[ (U + u_0) \frac{d\bar{\theta}}{d\xi} - \frac{d^2 \bar{\theta}}{d\xi^2} - \bar{\omega} \right] y - u_0 \left( \frac{d\bar{\theta}}{d\xi} \right) \frac{y^3}{3}. \tag{13}$$

When the boundary condition at  $y = 1$  is applied one finds

$$V \frac{d\bar{y}_F}{d\xi} - L_F^{-1} \frac{d^2 \bar{y}_F}{d\xi^2} = -\bar{\omega} \tag{14}$$

$$V \frac{d\bar{\theta}}{d\xi} - \frac{d^2 \bar{\theta}}{d\xi^2} = \bar{\omega} - \frac{\kappa \bar{\theta}}{\beta} \tag{15}$$

where  $V \equiv U + \frac{2}{3} u_0$  is the propagation speed relative to an observer moving with the average fluid velocity. These equations are identical to the equations describing the propagation of a planar flame with volumetric heat losses of intensity  $\kappa/\beta$ . The latter has been previously treated in the literature and possesses an analytical solution in the limit  $\beta \rightarrow \infty$ , which we summarize next.

For large activation energy the chemical reaction is confined to a thin region, located near  $\xi = 0$ , outside of which  $\bar{\omega}$  is exponentially small. The mass fraction of fuel and the temperature are therefore given by

$$\bar{y}_F = \begin{cases} 1 - \exp(VL_F \xi) & \xi < 0 \\ 0 & \xi > 0 \end{cases} \tag{16}$$

$$\bar{\theta} = \begin{cases} \bar{\theta}_f \exp \left\{ \frac{1}{2} [V + \sqrt{V^2 + 4\kappa/\beta}] \xi \right\} & \xi < 0 \\ \bar{\theta}_f \exp \left\{ \frac{1}{2} [V - \sqrt{V^2 + 4\kappa/\beta}] \xi \right\} & \xi > 0 \end{cases} \tag{17}$$

where  $\bar{\theta}_f$  denotes the temperature at the reaction sheet. Note that cooling in the post-reaction zone occurs on an  $\mathcal{O}(\beta)$  scale; namely much longer than the  $\mathcal{O}(1)$  preheat zone. A standard analysis of the reaction zone, c.f. [13–14] yields the relation

$$V = \exp(-h^*/2) \tag{18}$$

where  $h^* = \beta(\bar{\theta}_f - 1)$  is the drop in flame temperature from the adiabatic value. Note that, since in the limit considered the fuel is completely consumed, the propagation speed  $V$  is also the total burning rate (the dimensional propagation speed and burning rate, however, exhibit different dependence on the parameters). It is the only eigenvalue in this case, which can be determined from the integral relation

$$V = \frac{\kappa}{\beta} \int_{-\infty}^{\infty} \bar{\theta}(\xi) d\xi$$

that follows from Eq. 11. Using Eq. 17 and the relation (18) one finds, to leading order in  $1/\beta$ , the equation

$$V^2 \ln V = -\kappa$$

for  $V$ . The propagation speed  $V$  equals one for the adiabatic case ( $\kappa = 0$ ) and decreases with increasing values of  $\kappa$  until a critical value  $\kappa_{\text{ext}} = 1/2e \approx 0.18$  is reached. No solution exists for  $\kappa > \kappa_{\text{ext}}$  so that  $\kappa_{\text{ext}}$  represents the maximum allowable heat losses for flame propagation, or the extinction conditions. The propagation speed at extinction,  $V_{\text{ext}}$ , is given by

$$V_{\text{ext}} = e^{-1/2} \approx 0.607. \tag{20}$$

Although, for a given  $\kappa$ , Eq. 19 possesses a second solution with  $V < V_{\text{ext}}$ , it corresponds to an unstable state that cannot be realized physically.

The transverse variations in the fuel mass fraction and in temperature can now be obtained by integrating Eqs. 12 and 13 once more. In particular, if the preceding solution Eqs. 16 and 17 for large  $\beta$  is used along with the assumption<sup>2</sup> that  $L_F - 1 = \mathcal{O}(1/\beta)$ , one finds

$$y_F \sim \bar{y}_F(\xi) + \frac{1}{\epsilon^2} \left\{ \frac{u_0}{12} \left( \frac{d\bar{y}_F}{d\xi} \right) (2y^2 - y^4) + \psi_1(\xi) \right. \\ \left. + \mathcal{O}(\beta^{-1}) \right\} \tag{21}$$

$$\theta \sim \bar{\theta}(\xi) + \frac{1}{\epsilon^2} \left\{ \frac{u_0}{12} \left( \frac{d\bar{\theta}}{d\xi} \right) (2y^2 - y^4) + \psi_2(\xi) \right. \\ \left. - \frac{\kappa}{2\beta} \bar{\theta}(\xi) y^2 \right\} \tag{22}$$

where the functions  $\psi_i(\xi)$  can be determined by carrying the problem to the next order. Thus, in the absence of a flow, the flame (defined by the location of the reaction sheet) remains planar.

<sup>2</sup>A consistent asymptotic analysis of multi-dimensional flames with large activation energy requires that the Lewis number be retained near one, a formulation known as NEF [13].

With a flow, the flame curves and its shape is given by

$$\xi = \frac{u_0}{12\epsilon^2} (y^4 - 2y^2) \tag{23}$$

where, without loss of generality, we have set the constant  $\psi_1(0)$ , representing a translation along the axis, to zero. Note that the flame is concave/convex towards the unburned gas at the center of the channel, depending on whether  $u_0$  greater/less than zero, as shown in the sketch of Fig. 1.

In summary, in a frame of reference moving with the average flow velocity, the mean temperature and concentration profiles in narrow channels are identical to those obtained by solving a one-dimensional problem with volumetric heat losses of intensity  $\kappa$ . The total burning rate  $\Omega = V$  with  $V$  given by Eq. 19; it depends only on the parameter  $k\epsilon^2$  and, to leading order, is independent of the flow velocity. The propagation speed  $U = V - \frac{2}{3}u_0$  indicating that the flame moves slower when opposed by the flow and can be blown off for sufficiently large  $u_0$ ; see also the discussion in [7]. Total flame extinction can be brought about when the parameter  $k\epsilon^2$  is larger than a critical value, which for large activation energy chemical reactions is about  $1/2e \approx 0.18$ . This condition provides the maximum heat losses allowable for flame propagation in a channel of given width, or the minimum channel width that permits flame propagation for a prescribed magnitude of heat losses. Finally, we note that in narrow channels the effects due to non-unity Lewis numbers are secondary and will not be further pursued here.

**MODERATE AND WIDE CHANNELS—  
NUMERICAL RESULTS**

The two-dimensional problem consisting of Eqs. 2 and 3 and boundary conditions Eqs. (4) and (6) was solved numerically with  $\beta = 8$  and  $\alpha = 0.85$ . The focus has been to examine the influence of heat losses on flame propagation in channels of various widths both in a quiescent mixture and in the presence of a Poiseuille flow. Thus, variations in the three parameters  $\epsilon$ ,  $u_0$ , and  $k$  are considered while for simplicity we

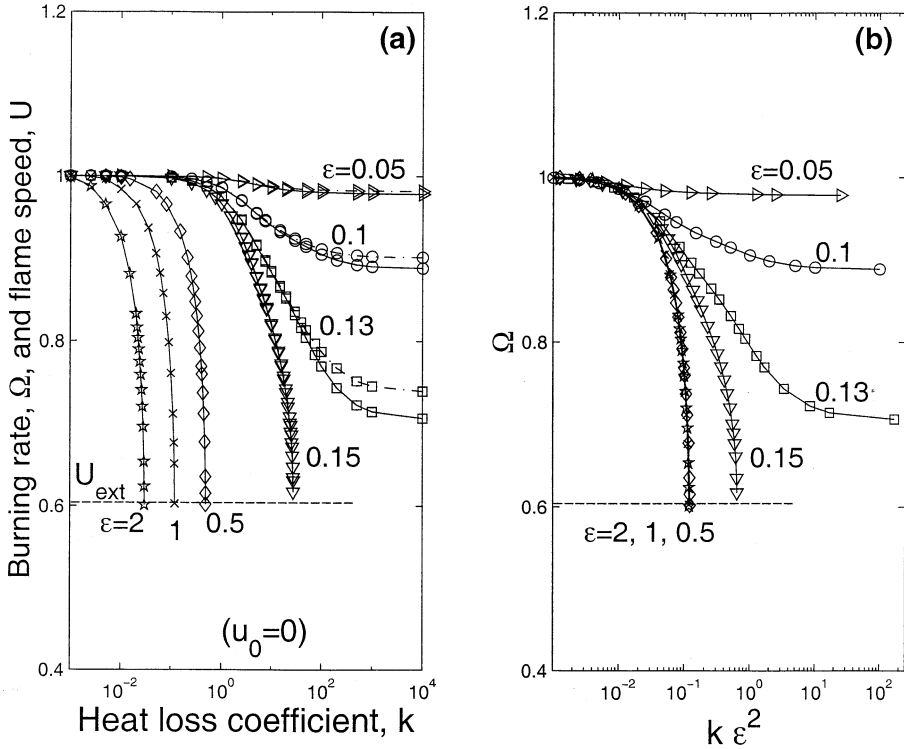


Fig. 2. Burning rate  $\Omega$  (solid line) and propagation speed  $U$  (dash-dotted line) plotted against (a) the heat loss coefficient  $k$ , and (b) the parameter  $\kappa = k\epsilon^2$ . (Note that the curves for  $\Omega$  and  $U$  are almost indistinguishable except for the lower values of  $\epsilon$ ). The various curves correspond to different values of  $\epsilon$ , which is the reciprocal of the channel half-width in units of the laminar flame thickness. The calculations in this graph pertain to  $u_0 = 0$ . The horizontal dotted line corresponds to the asymptotic prediction,  $U_{ext} \approx 0.607$ , valid for  $\epsilon \gg 1$ .

assumed a unity Lewis number,  $L_F = 1$ . Non-unity Lewis number effects will be treated in a sequel. Similar to our previous study [7], the numerical procedure is based on a finite-volume discretization of the steady equations over a rectangular but nonuniform grid, with typically  $8 \cdot 10^4$  points. An iterative procedure is used with the propagation speed  $U$  updated so as to keep the flame at a fixed location in the computational domain. The dimensions of the latter are typically 1 in the  $y$ -direction and  $500\epsilon$  in the  $x$ -direction (in terms of the reference units).

It should be emphasized that in the reported calculations the propagation speed  $U$  and burning rate  $\Omega$  have been re-normalized by the corresponding value of the planar adiabatic flame obtained numerically for  $\beta = 8$ , which differs from the asymptotic values that are, strictly speaking, valid only when  $\beta \rightarrow \infty$ .

**Quiescent Mixture**

We first consider the case of no imposed flow; that is  $u_0 = 0$ . The main results are summarized in Fig. 2a where the burning rate  $\Omega$  and propagation speed  $U$  are plotted against the heat loss parameter  $k$  for selected values of  $\epsilon$ . The burning rate is represented by solid lines and the propagation speed by dash-dotted lines, but they are indistinguishable except for large values  $k$  in relatively wide channels where fuel leakage occurs near the walls with residual fuel left behind ( $y_{F_w} \neq 0$ ). Note from Eq. 8 that  $\Omega = U(1 - y_{F_w})$  so that, for given  $\epsilon$  and  $k$ , the difference between the two curves is proportional to  $y_{F_w}$ . All curves asymptote to 1 when  $k \rightarrow 0$ , as they should. For  $k > 0$  the figure clearly identifies the existence of two regimes, depending on the value of  $\epsilon$ .

1. In relatively narrow channels corresponding to  $\epsilon$  larger than a threshold value  $\epsilon_*$ , total extinction is brought about as  $k$  is increased above an extinction value. The threshold value is determined numerically to be  $\epsilon_* \approx 0.135$ . This implies that total extinction by excessive losses may be expected only if the channel-width is smaller than the critical distance  $(2/\epsilon_*)\ell_F$  which is about 15 times the laminar flame thickness  $\ell_F$ . The propagation speed at extinction is slightly below 0.6, which is very close to the asymptotic prediction,  $U_{\text{ext}} \approx 0.607$ , valid for narrow channels. As noted, the burning rate and propagation speed in the limit  $\epsilon \gg 1$  depend on the parameter  $k\epsilon^2$  which can be verified here by replotting the numerical results accordingly, as shown in Fig. 2b. The curves corresponding to  $\epsilon = 2$ ,  $\epsilon = 1$  and even that for  $\epsilon = 0.5$ , collapse into a single curve when plotted against  $k\epsilon^2$ . Extinction in this regime occurs for  $k\epsilon^2$  equal to about 0.12, to be compared to the asymptotic value 0.18 obtained in the limit of large activation energy. As  $\epsilon$  approaches the threshold value  $\epsilon_*$ , the critical value of  $k\epsilon^2$  increases; for  $\epsilon = 0.15$ , for example, total extinction occurs only when  $k\epsilon^2$  reaches the value 0.63 (or  $k \approx 28$ ).

Temperature and reaction rate contours across half the channel are shown in Fig. 3 for  $\epsilon = 0.15$  and several values of  $k$ , increasing from top to bottom. For each case five reaction rate iso-contours, corresponding to five values of  $\omega$  distributed between 0 and  $\omega_{\text{max}}$ , and five temperature iso-contours, corresponding to five values of  $\theta$  distributed between 0 and  $\theta_{\text{max}}$ , are presented; the values of  $\omega_{\text{max}}$  and  $\theta_{\text{max}}$  are indicated for each case. For the adiabatic case ( $k = 0$ ) the flame is planar and extends all the way to the wall; the maximum temperature is the adiabatic flame temperature  $\theta = 1$ . When  $k$  is increased the flame extinguishes near the walls and retracts towards the centerline. Total flame extinction occurs when  $k$  exceeds the critical value  $k_{\text{ext}} \approx 28.1$ . We note that since the channel is relatively narrow, heat losses practically affect the temperature across the whole gap. Indeed the maximum temperature in the channel, for near-extinction conditions, is  $\theta_{\text{max}} = 0.94$ , compared to the adiabatic tem-

perature  $\theta = 1$ . Although this appears to be a modest drop, it is sufficient to bring about total flame extinction since the Zeldovich number,  $\beta = 8$ , is quite large. Note that the fuel that escapes through near the walls is being depleted in the relatively hot region behind the reaction zone (see also Fig. 2a).

2. In relatively wider channels,  $\epsilon < \epsilon_*$ , the flame can only experience partial extinction. This is illustrated in Fig. 4 for the case  $\epsilon = 0.1$  where, similar to Fig. 3, temperature and reaction rate contours are plotted for several values of  $k$ . For the adiabatic case the flame again spans the whole channel but is significantly thinner. When  $k$  is increased, the flame extinguishes near the walls and retracts towards the centerline. Combustion persists for arbitrary large values of  $k$ ; the limit  $k \rightarrow \infty$  corresponds to cold walls that are maintained at the same temperature as the fresh unburned gas; that is  $\theta_{\text{wall}} = 0$ . Because the channel is wide enough, burning can persist near the center with the temperature falling off to the ambient value near the walls, as well as far upstream. For this reason, the temperature in the reaction zone at the center of the channel reaches the adiabatic flame temperature  $\theta = 1$ , in contrast to the results depicted in Fig. 3. The dead-space, namely the distance near the wall where the flame is quenched, can be as large as five times the flame thickness  $\ell_F$  this is close to the experimentally reported values [4, 11], which are of order 6. Finally we note that the fuel that escapes near the walls is at a relatively low temperature so that it remains unburned with the residual determined from  $y_{F_\infty} = 1 - \Omega/U$  (see also Fig. 2a).

Figure 5 shows the dependence of the burning rate and propagation speed on  $\epsilon$  for selected values of  $k$ . Again we note that  $\Omega$  and  $U$  are almost indistinguishable. For fixed  $k$ , these quantities decrease with increasing  $\epsilon$  since the heat loss per unit volume  $\sim k\epsilon^2$  increases. The curve labeled  $k = \infty$ , corresponding to cold wall conditions is of particular significance. It gives the minimum allowable speed in presence of conductive heat losses in terms of the channel width  $\sim 2\epsilon^{-1}$ . It also gives the smallest channel



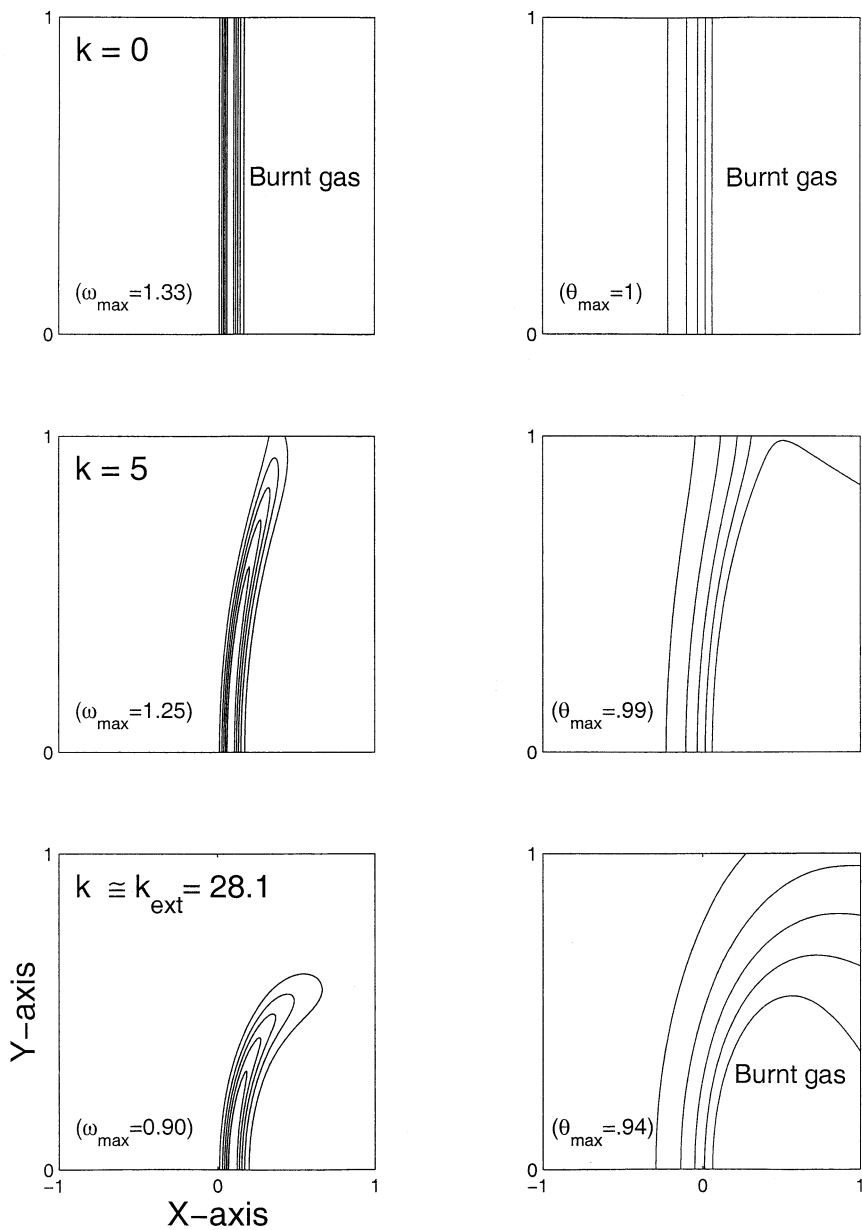


Fig. 3. Reaction rate  $\omega$  and temperature  $\theta$  iso-contours for the case  $\epsilon = 0.15$  with no flow ( $u_0 = 0$ ). The subfigures on the left correspond to five values of  $\omega$  distributed between 0 and  $\omega_{\max}$  and those on the right to five values of  $\theta$  distributed between 0 and  $\theta_{\max}$ ; the values of  $\omega_{\max}$  and  $\theta_{\max}$  are indicated in each subfigure. Total extinction occurs for a value of  $k$  slightly larger than  $k_{\text{ext}}$ .

width permitting flame propagation if the walls are kept at the temperature of the fresh mixture. This distance, denoted by  $d_q$  is known as the quenching distance (between parallel plates). Experimentally reported values of  $d_q$ , measured in units of the planar flame thickness,

are in the range 10 to 30, depending on the mixture and the equivalence ratio; see for example [3, 15]. Our numerical value is  $d_q \approx 15$  is well within this range. Clearly the quenching distance is smaller for finite values of  $k$  and is zero if the walls are strictly adiabatic.

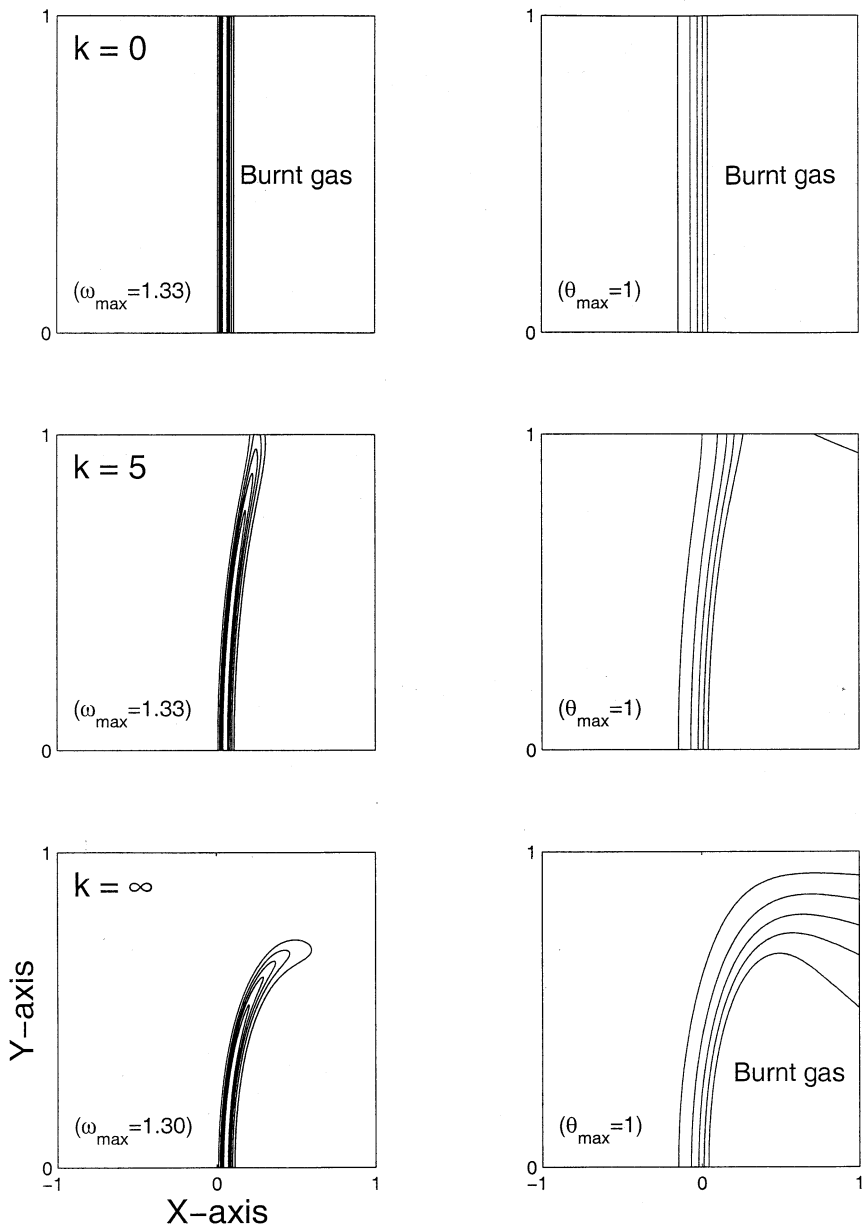


Fig. 4. Reaction rate  $\omega$  and temperature  $\theta$  iso-contours, similar to Fig. 3, but with  $\epsilon = 0.1$ . The bottom case, calculated with the boundary condition  $\theta = 0$  at the walls, simulates an infinite value of  $k$ .

**Propagation in the Presence of Flow**

To describe the influence of a flow field on combustion in the presence of heat losses, the analysis of last section will be repeated with  $u_0 \neq 0$ . We examine both the case  $u_0 > 0$  where the flow is directed towards the burned gases, and  $u_0 < 0$ , for which it is directed towards the unburned gas.

A comparative presentation of results is reported in Fig. 6 for  $u_0 = 0.5$ ,  $u_0 = 0$ , and  $u_0 = -0.5$ . In each subfigure the burning rate  $\Omega$  is plotted versus  $k$  for selected values of  $\epsilon$ . In all three cases considered the flame propagates to the left, since  $U > 0$  as can be easily verified from Eq. 8 along with the data reported in the figure. We note parenthetically that for sufficiently large positive values of  $u_0$  the flame can

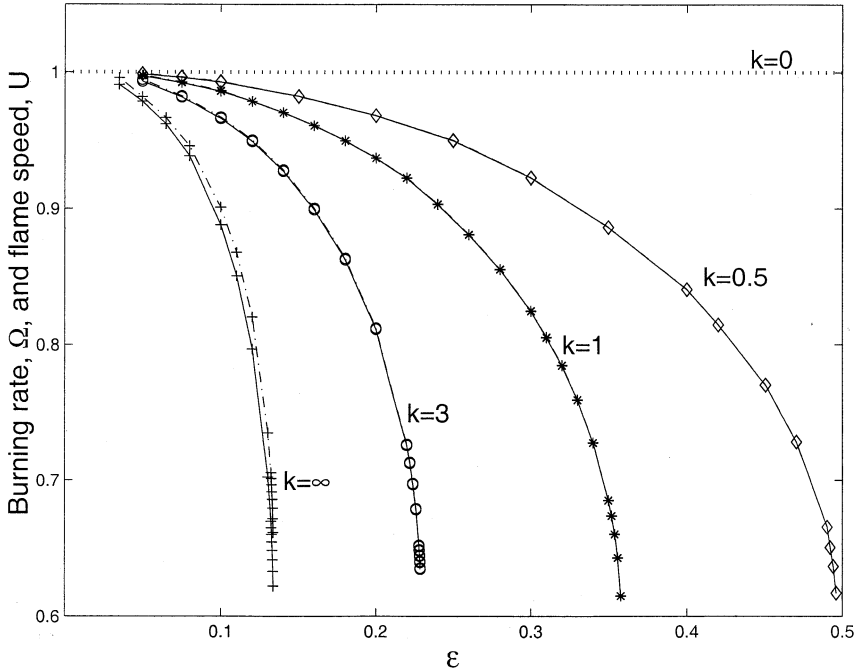


Fig. 5. Burning rate  $\Omega$  (solid line) and propagation speed  $U$  (dash-dotted line) plotted against  $\epsilon$  for selected values of  $k$ , with no flow ( $u_0 = 0$ ). For a given  $k$ , solutions exist only for  $\epsilon < \epsilon^*$  which determines the quenching distance.

be blown off by the flow, thus traveling as a whole to the right ( $U < 0$ ). The critical value,  $u_0^{cr}$  say, corresponding to  $U = 0$  is the condition necessary to stabilize the flame; blowoff occurs for  $u_0 > u_0^{cr}$ . The possibility of a flame being blown off diminishes as  $\epsilon$  decreases and when fuel leakage increases.

The main conclusion drawn from Fig. 6 is that the flame is more sensitive to heat losses when it is opposed by the flow ( $u_0 > 0$ ) and less sensitive when it is assisted by it ( $u_0 < 0$ ). For example, for  $\epsilon = 0.13$  heat losses at the wall are able to cause total extinction when  $u_0 = 0.5$  while this is impossible when  $u_0 = 0$  or  $u_0 = -0.5$ . Also, for  $\epsilon = 0.15$ , total quenching is impossible when  $u_0 = -0.5$  but possible for  $u_0 = 0$  or  $u_0 = 0.5$ . In short, the range of channel widths allowing total extinction is widened as  $u_0$  increases from negative to positive values. It can be also noted that the dependence of the burning rate  $\Omega$  on the flow is unnoticeable in narrow channels as seen by comparing the three curves corresponding to  $\epsilon = 2, 1,$  and  $0.5$ ; these curves would have collapsed into a single curve had we plotted  $\Omega$  against  $k\epsilon^2$ . This behavior is consistent with the asymptotic predictions which show that, to lead-

ing order, the burning rate depends only on  $k\epsilon^2$  (and not on  $u_0$ ).

For small  $\epsilon$ , we expect the flame to deviate from the adiabatic case only in a region near the wall whose size, of the order of the planar flame thickness, tends to zero as  $\epsilon \rightarrow 0$ . Hence the (global) burning rate  $\Omega$  would be negligibly affected by the wall boundary condition in this limit and would approach that of the adiabatic case. This is confirmed in Fig. 7 where the burning rate is plotted against  $\epsilon$  for selected values of  $k$  and for the three values of  $u_0$  under consideration. The asymptotic approach to the adiabatic curves, labeled  $k = 0$ , is clear. In [7] we have derived the following expressions for the burning rate valid in the adiabatic case and for  $\epsilon \ll 1$ :

$$\Omega \sim \begin{cases} 1 + \frac{2}{3}u_0 - 2.04 \cdot (u_0\epsilon)^{2/3} & u_0 > 0 \\ 1 - \frac{1}{3}u_0 - \sqrt{-2u_0}\epsilon & u_0 < 0 \end{cases} \quad (24)$$

The solid curves intersecting the vertical axis in the upper and bottom subfigures are based on

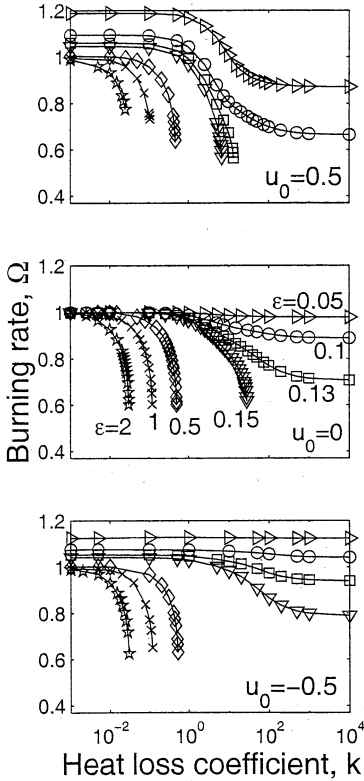


Fig. 6. Burning rate  $\Omega$  plotted against the heat loss coefficient  $k$  for selected values of  $\epsilon$  and for the three cases:  $u_0 = 0.5$ ,  $u_0 = 0$ , and  $u_0 = -0.5$ .

these expressions and are seen to agree very well with the numerically calculated values. This figure also provides, for given  $k$ , the dependence of the quenching distance on the flow and, as seen,  $d_q$  increases with increasing  $u_0$  (from negative to positive values).

The coupled influence of the flow and heat loss on the flame is further illustrated in the next four figures, which are similar to Figs. 3 and 4 except that  $u_0 = 0.5$  for the first two and  $u_0 = -0.5$  for the last ones. Fig. 8 corresponds to  $\epsilon = 0.15$  which is a relatively narrow channel; the flame here spans almost its entire width. Total extinction occurs for a value of  $k$  slightly larger than 6.7. In Fig. 9, corresponding to  $\epsilon = 0.1$ , the flame persists even for  $k = \infty$  showing that this case belongs to the regime where only partial extinction is possible. We note that in both cases the flame shape, for the adiabatic case and for small values of  $k$ , is similar to that predicted by Eq. 23. For larger values of  $k$  heat losses cause

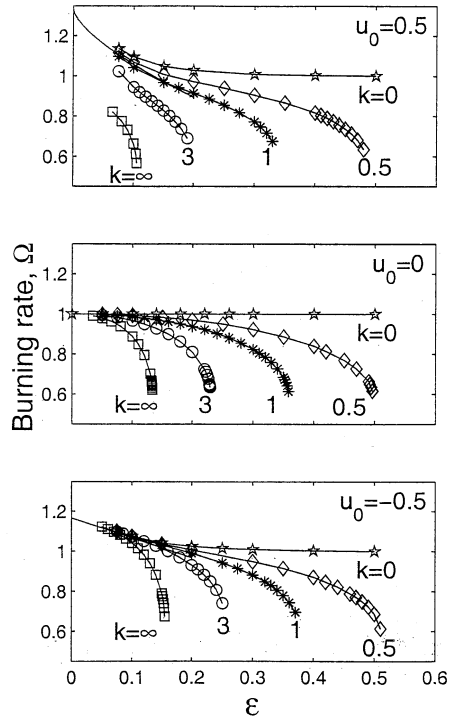


Fig. 7. Burning rate  $\Omega$  plotted against  $\epsilon$  for selected values of  $k$  and for the three cases:  $u_0 = 0.5$ ,  $u_0 = 0$ , and  $u_0 = -0.5$ .

a significant drop in temperature near the walls and the flame, limited to the center of the tube, takes on a convex shape with its leading edge along the centerline. The equivalent figures, Figs. 10 and 11, corresponding respectively to  $\epsilon = 0.15$  and 0.1 with  $u_0 = -0.5$  show that in both cases total extinction is not possible no matter how large  $k$  is. Here too the flame shape, for the adiabatic case and for small values of  $k$ , is similar to that predicted by Eq. 23. For larger values of  $k$  the flame is limited to the center of the tube.

Figure 12 provides a summary of extinction results for the three cases just discussed. We have plotted in this figure the value of  $\epsilon^2 k_{\text{ext}}$  with  $k_{\text{ext}}$  the value of the heat loss coefficient at extinction, as a function of the channel-half width  $\sim \epsilon^{-1}$ , for  $u_0 = -0.5$ ,  $u_0 = 0$ , and  $u_0 = 0.5$ . The three curves tend to a constant limit as the channel width is decreased; the limit corresponds to  $\epsilon^2 k_{\text{ext}} = 0.12$  which is close to the asymptotic prediction of 0.18 obtained in the limit  $\epsilon \rightarrow 0$ . Each curve admits a vertical asymptote that determines the channel half-width

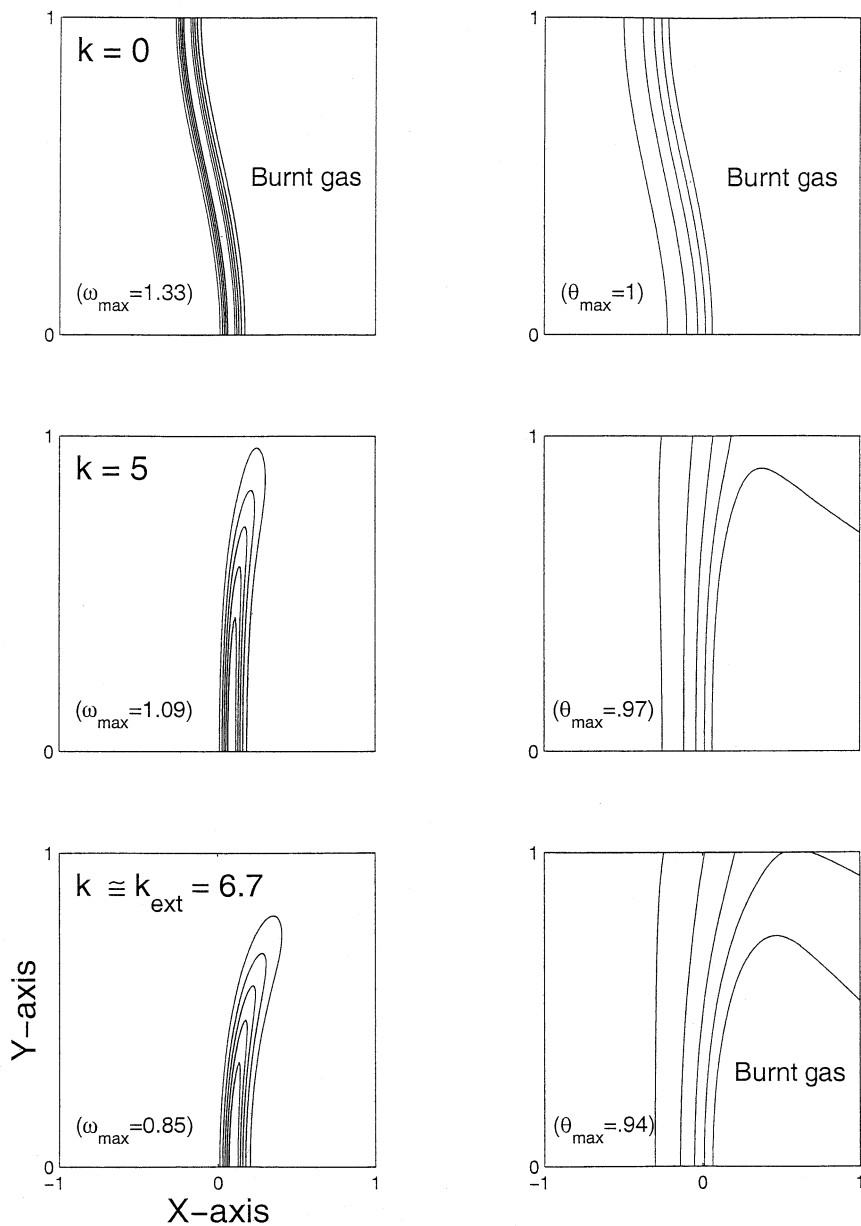


Fig. 8. Reaction rate  $\omega$  and temperature  $\theta$  iso-contours, similar to Fig. 3, but with  $\epsilon = 0.15$  and with a flow corresponding to  $u_0 = 0.5$ .

corresponding to total extinction. This value, related to the quenching distance  $d_q$  is seen to increase with increasing  $u_0$  as noted earlier. Each curve also separates a region where no flame may exist (above the curve) from a region where only partial quenching is possible (below and to the right of the curve).

**Cold walls**

In this section we present a synthesis of results for the most severe case of heat losses, namely for the case where the walls are held at the temperature of the fresh mixture ( $k \rightarrow \infty$ ). In practice this is achieved by cooling the walls and

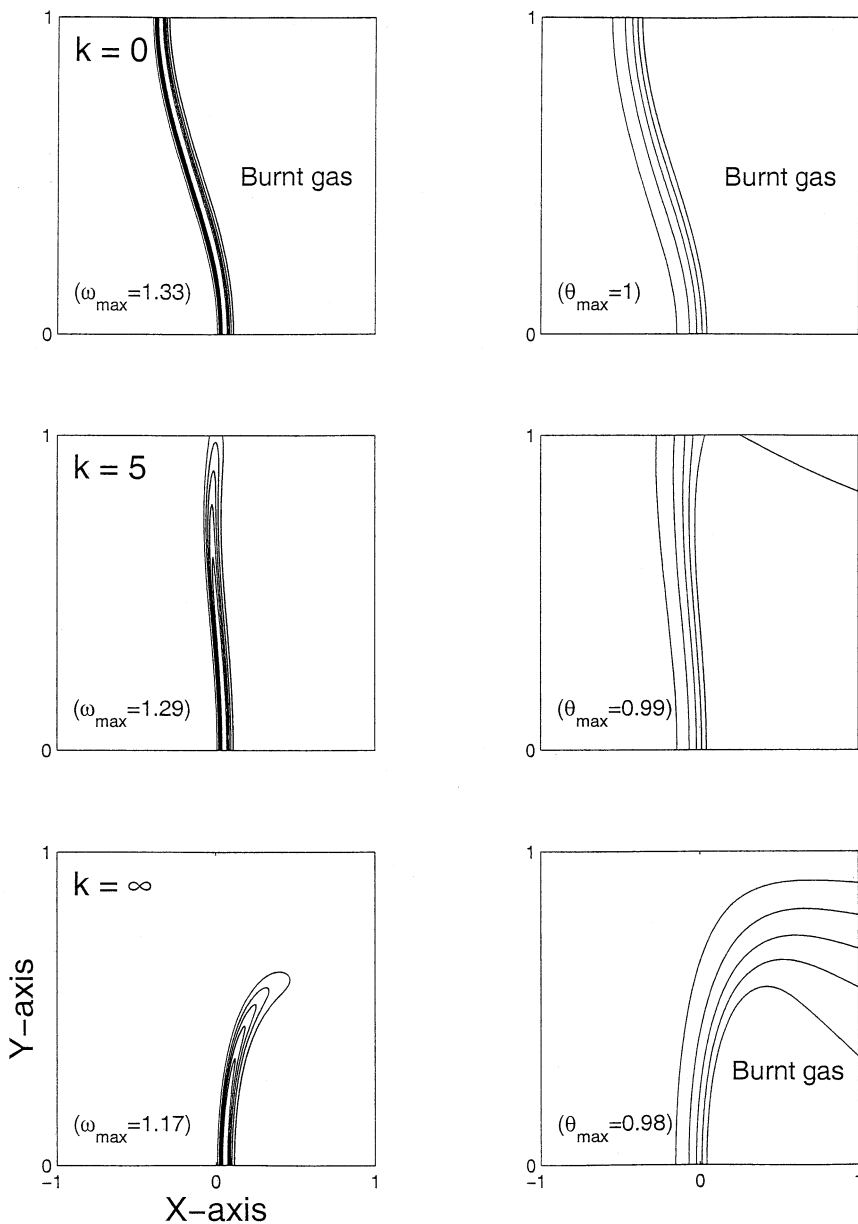


Fig. 9. Reaction rate  $\omega$  and temperature  $\theta$  iso-contours, similar to Fig. 3, but with  $\epsilon = 0.1$  and with a flow corresponding to  $u_0 = 0.5$ .

values of quenching distances in the literature generally refers to this configuration, but with no external flow. Our main aim here is to determine the magnitude of the quenching distance with and without flow.

Shown in Fig. 13 is the burning rate  $\Omega$  versus  $\epsilon$  for selected values of  $u_0$ , positive and negative. Each curve is seen to admit a turning point for

a specific value of  $\epsilon$ , say  $\epsilon_{ext}$ . This value determines the quenching distance  $d_q \sim 2\epsilon_{ext}^{-1}$  in units of the laminar flame thickness  $\ell_F$ . The variation of  $\epsilon_{ext}$  with  $u_0$  is reported in Fig. 14. It is seen that  $\epsilon_{ext}$  decreases with increasing  $u_0$ , translating an increased sensitivity of the flame to heat losses. For example, for  $u_0 = 1$  the flame persists only if the channel width is larger than

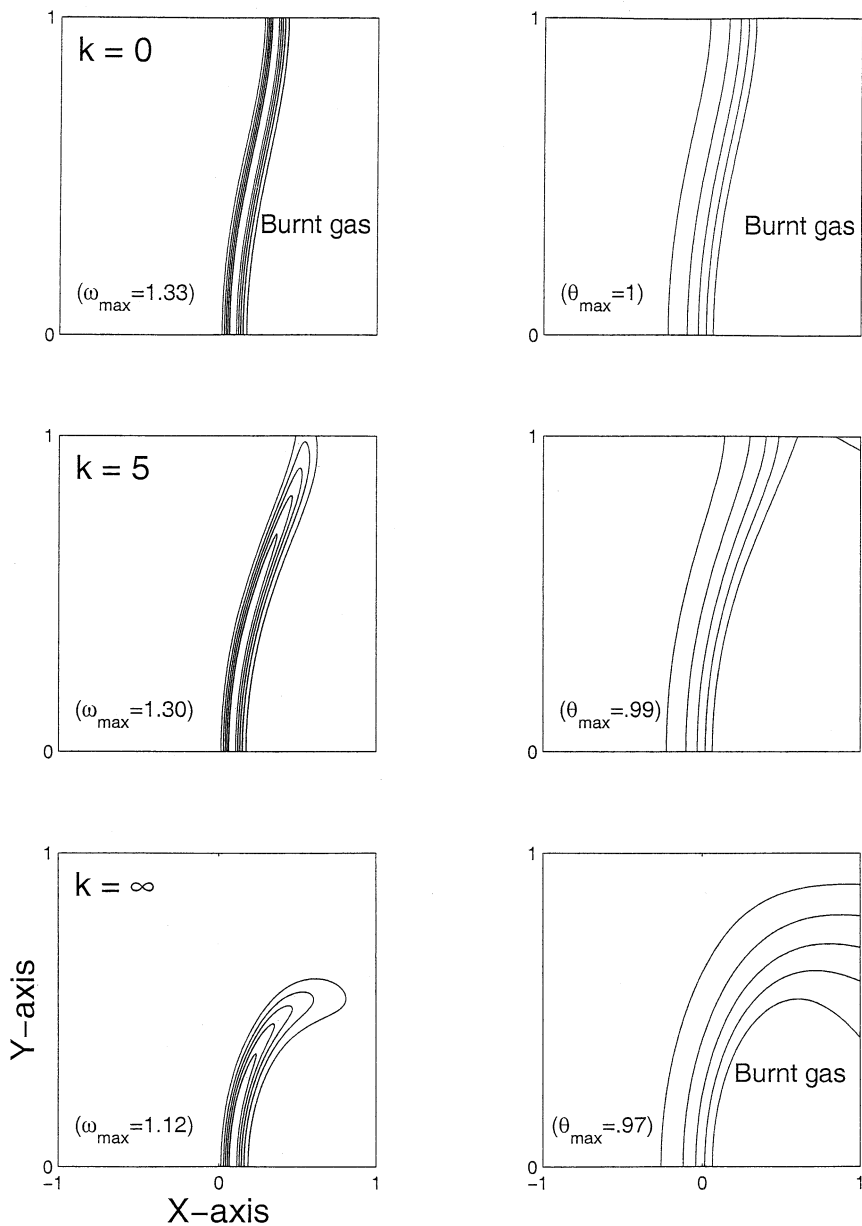


Fig. 10. Reaction rate  $\omega$  and temperature  $\theta$  iso-contours, similar to Fig. 3, but with  $\epsilon = 0.15$  and with a flow corresponding to  $u_0 = -0.5$ .

about  $30\ell_F$ ; this is to be compared to about  $15\ell_F$  in the stagnant case and  $12\ell_F$  for  $u_0 = -1$ . Moreover, the curve delimits two regions in the  $\epsilon-u_0$  plane: in the region above the curve no flame is possible while in the region below the curve only partial extinction occurs with the flame persisting in the center of the channel. It is interesting to obtain the value of  $u_0^*$  corre-

sponding to the limit  $\epsilon_{\text{ext}} \rightarrow 0$ . This value is difficult to obtain numerically, but can be estimated by extrapolating the extinction curve to  $\epsilon = 0$  (the dotted segment shown in the figure). We find that  $u_0^* \approx 1.5$  in this limit, or  $2u_0^*/3 \approx 1$ . Because  $2u_0/3$  is the average flow velocity in the channel we conclude that no flame, however thin, is able to survive if the average flow speed

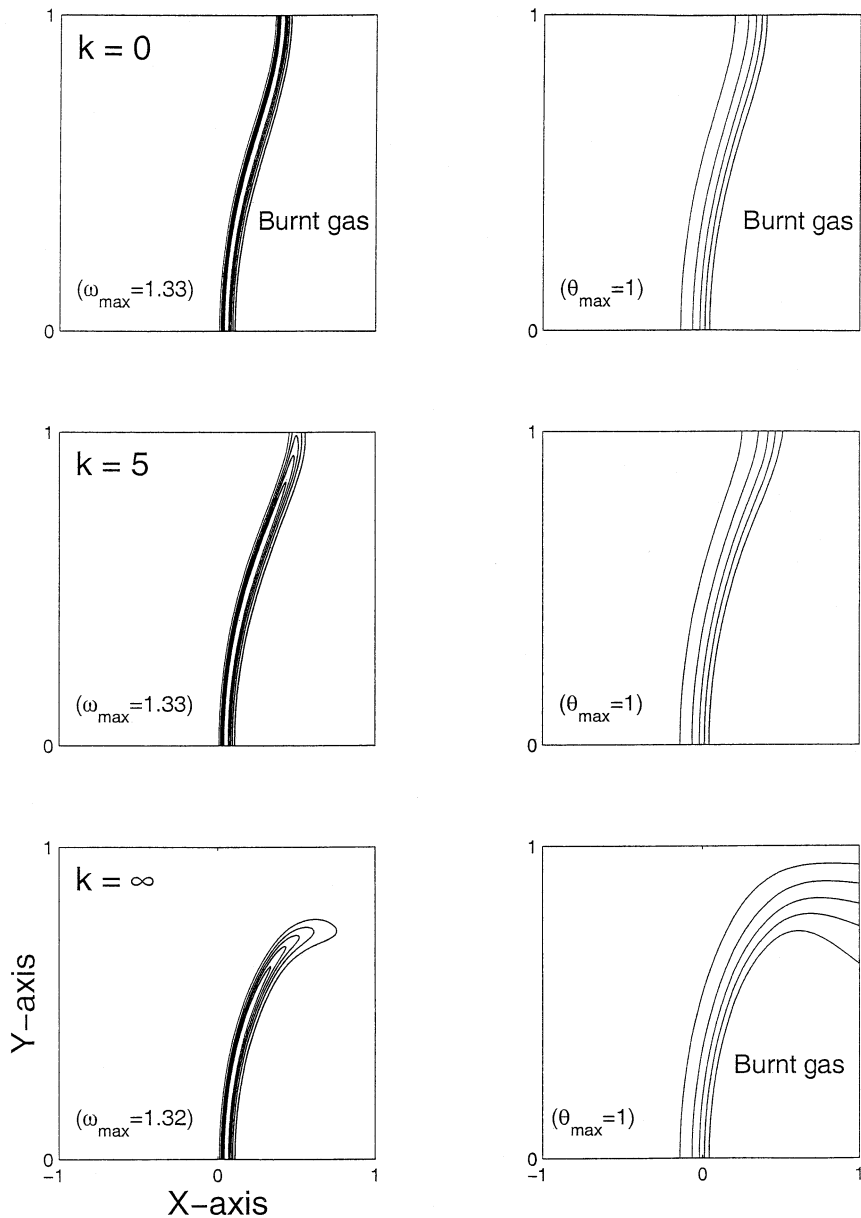


Fig. 11. Reaction rate  $\omega$  and temperature  $\theta$  iso-contours, similar to Fig. 3, but with  $\epsilon = 0.1$  and with a flow corresponding to  $u_0 = -0.5$ .

is larger than about one (the laminar flame speed). Thus, as a result of heat losses, flame flashback will not occur in a channel if the walls are held at the temperature of the cold combustible mixture and the average flow speed is larger than the laminar flame speed. This is in marked contrast with the opposite extreme case

of an adiabatic channel discussed in [7]. For the adiabatic case the flame will always flashback, irrespective of the flow, in the limit  $\epsilon \rightarrow 0$ . For a finite fixed value of  $\epsilon$ , however, conditions ensuring non-occurrence of flashback in an adiabatic channel can be determined (see discussion of Fig. 7 in [7]).



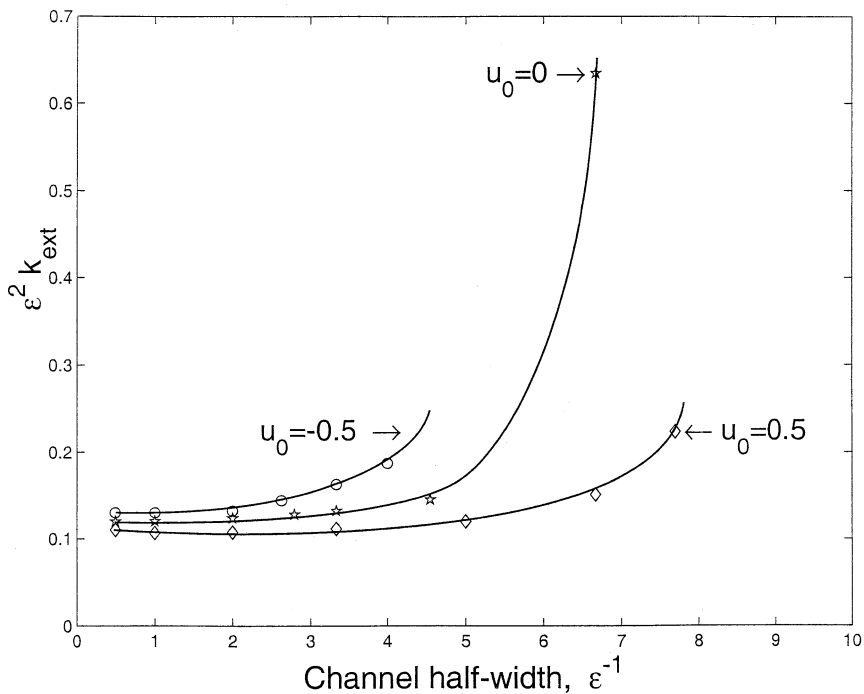


Fig. 12. The dependence of  $\epsilon^2 k_{\text{ext}}$  on the channel-half width  $\sim \epsilon^{-1}$ ; here  $k_{\text{ext}}$  is the value of the heat loss coefficient at extinction. The three curves correspond to  $u_0 = 0.5, u_0 = 0$ , and  $u_0 = -0.5$ .

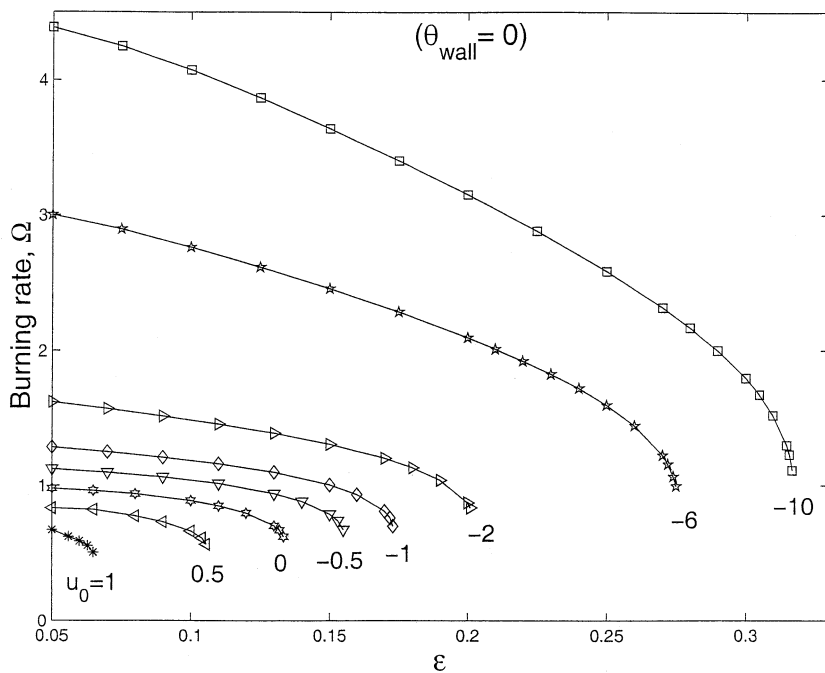


Fig. 13. Burning rate  $\Omega$  plotted against  $\epsilon$  for selected values of  $u_0$ , corresponding to the “cold walls” boundary conditions.

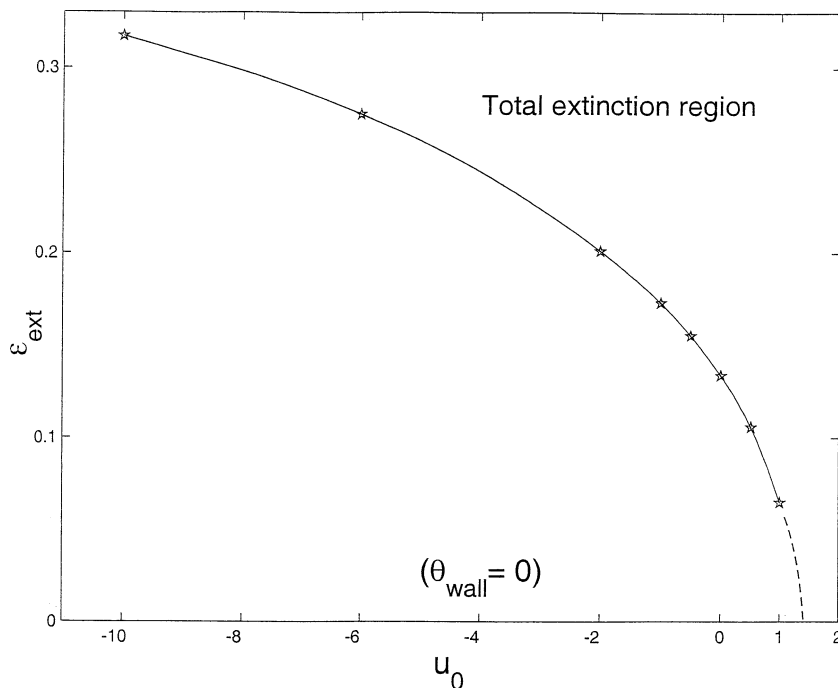


Fig. 14. Extinction curves for the case of cold walls. The curve that determines the dependence of  $\epsilon_{\text{ext}}$  on  $u_0$  separate a region where no flame can propagate from a region where only partial extinction is possible.

## CONCLUSIONS

We have described flame propagation in a channel subject to a Poiseuille flow and conductive heat losses to the walls. The study has focused on the influence of the flow strength, the heat loss intensity, and the channel width on the global burning rate. Two modes of extinction have been described: total flame extinction in narrow channels and partial flame extinction in wider channels. In narrow channels total flame extinction may be brought about by excessive losses. The magnitude of the losses is proportional to the square of the channel's width, with extinction occurring when the burning rate is approximately  $0.6S_L$ . These conclusions, obtained from numerical calculations with finite rate chemistry, are well captured by the classical result of a one-dimensional flame with volumetric heat losses  $\sim (\ell_F/a)^2$ . Our prediction of the quenching distance  $d_q \sim 15\ell_F$  is in accord with experimental values. In moderate and wide channels only partial flame extinction is possible. Burning persists near the center of the channel, even for cold walls, with the tempera-

ture falling off rapidly on both sides to that of the fresh mixture. The dead space near the walls is of the order of  $6\ell_F$ , namely significantly smaller than half the quenching distance. This observation is also in general agreement with experimentally reported values [3]. In the presence of a flow, it was found that when directed from the unburned towards the burned gas the flame is more vulnerable to heat losses while when directed towards the fresh unburned mixture it is less sensitive. In particular, the quenching distance increases by increasing the mean flow rate, when the flame is opposed by the flow, similar to the observations reported in [15] where the strength of the flow was increased by increasing its turbulent intensity. Finally, special attention has been devoted to the practical case of cold-walls, for which the regions of total and partial extinction regimes have been mapped in terms of the flow strength and the channel width.

It will be interesting to assess the influence of thermal expansion on the extinction characteristics examined here, particularly in wide channels where its influence is expected to be of

greater significance. The induced transverse flow towards the axis of the channel, resulting from the segments of the flame that are nearly parallel to the walls, is quickly redirected by the imposed flow increasing the mean flow rate in the channel. Based on the present work, it may be anticipated therefore that this would cause an increase in the sensitivity of the flame to extinction. On the other hand, thermal expansion weakens the gradients in the vicinity of the flame which may have an adverse effect.

*This work has been supported partially by the National Science Foundation and by NASA Microgravity Combustion Research.*

## REFERENCES

1. Heywood, J. B., *Internal Combustion Engine Fundamentals*, McGraw-Hill Publishing Company, New York, 1988.
2. Von Karman, T., and Millan, G., *Proceedings of the Combustion Institute*, 4:173, 1953.
3. Ferguson, C. R., and Keck, J. C. *Combust. Flame* 28:197 (1977).
4. Clendening, J. C., Shackelford, W., and Hilyard, R., *Proceedings of the Combustion Institute* 18:1583 (1981).
5. Lu, J. H., Ezekoye, R., and Sawyer, R. F., *Proceedings of the Combustion Institute* 23:441, 1990.
6. Lewis, B., and Von Elbe, G. *Combustion, Flames and Explosions of Gases*, Academic Press, 1961.
7. Daou, J., and Matalon, M., *Combust. Flame* 124:337 (2001).
8. Benkhaldoun, F., Larrourou, B., and Denet, B., *Combust. Sci. and Tech.* 64:187 (1989).
9. Barenblatt, G. I., Zeldovich, Y. B., and Istratov, A. G., *Prikl. Mekh. Tekh. Fiz.* 2, 21, (1962).
10. Carrier, G. F., Fendell, F. E., and Feldman, P. S., *Proceedings of the Combustion Institute* 20:67 (1984).
11. Fairchild, P. W., Fleeter, R. D., and Fendell, F. E., *Proceedings of the Combustion Institute* 20:85 (1984).
12. Matalon, M., and Daou, J., *AIAA Paper 2001-0949. Presented at 39th AIAA Aerospace Sciences Meeting & Exhibit*, January 2001.
13. Buckmaster, J., and Ludford, G. S. S., *Theory of Laminar Flames*, Cambridge, 1982.
14. Williams F. A., *Combustion Theory*, Menlo Park, CA, 1985.
15. Ballal D. R., and Lefebvre, A., *Proceedings of the Royal society of London A.* 357:163 (1977).

*Received 12 March 2001; revised 2 November 2001; accepted 12 November 2001*